Near-Field Optics: Microscopy, Spectroscopy, and Surface Modification Beyond the Diffraction Limit

Eric Betzig and Jay K. Trautman

The near-field optical interaction between a sharp probe and a sample of interest can be exploited to image, spectroscopically probe, or modify surfaces at a resolution (down to ~12 nm) inaccessible by traditional far-field techniques. Many of the attractive features of conventional optics are retained, including noninvasiveness, reliability, and low cost. In addition, most optical contrast mechanisms can be extended to the near-field regime, resulting in a technique of considerable versatility. This versatility is demonstrated by several examples, such as the imaging of nanometric-scale features in mammalian tissue sections and the creation of ultrasmall, magneto-optic domains having implications for high-density data storage. Although the technique may find uses in many diverse fields, two of the most exciting possibilities are localized optical spectroscopy of semiconductors and the fluorescence imaging of living cells.

Optical microscopy is such a pervasive technology that it is easy to take its impact for granted. On the scientific end, its applicability ranges from the imaging of living specimens, to the characterization of advanced materials, to the spectroscopic analysis of semiconductors. On the technological side, optics lies at the heart of integrated circuit fabrication processes and is central to the operation of commercial compact disc players and new, high-density data storage devices. In these and other applications (*1*), there is a growing need for higher spatial resolution, either to extract more information from, or to compress it into, a given area. Unfortunately, conventional optics will have a diminishing importance as the problems of interest push further into the nanometric regime, because the limit of its resolution, as originally determined by E. Abbe (*2*), is only ~$\lambda/2$ or ~200 nm for visible light (λ is the wavelength of light).

The techniques that, by virtue of their capability for producing superior resolution, stand ready to take over under these circumstances fall into two broad classes. The first involves the use of shorter wavelength radiation, such as in electron or x-ray microscopy (*3*, *4*). The second includes the various forms of scanning probe microscopy (*5*), of which scanning tunneling microscopy (STM) (*6*) is the best known example. That these methods have not already largely supplanted optical microscopy is attributable to the fact that, in the quest for higher resolution, a faustian bargain has been struck so that in each method, several of the attractive features of optical microscopy have been sacrificed, such as nondestructiveness, low cost, high speed, reliability, versatility, accessibility, ease of use, and informative contrast. It is therefore clear that much can be gained by combining the interaction mechanisms of optical microscopy with the high resolution of the scanning probe methods. The goal of this article is to demonstrate that the resulting technique, near-field scanning optical microscopy (NSOM) (*7*), is sufficiently powerful to have an impact in many different disciplines.

The authors are at AT&T Bell Laboratories, Murray Hill, NJ 07974.

The Near-Field Concept

Fourier optics can be used (*8*, *9*) to demonstrate easily that the diffraction limit to resolution in optical microscopy is not fundamental but rather arises from the assumption that the detection element (that is, a lens) is typically many wavelengths away from the sample of interest. However, by laterally scanning a source or detector of light in close proximity to the sample, one can generate an image at a resolution functionally dependent on only the probe size and the probe-to-sample separation, each of which can, in principle, be made much smaller than the wavelength of light. Perhaps the easiest such probe to conceptualize, and certainly the first one to be proposed (*10*, *11*), consists of a subwavelength-diameter aperture in an optically opaque screen (Fig. 1A). Light incident upon one side of the screen is transmitted through the aperture and, if the sample is within the near field, illuminates only one small region at any one time. The validity of this concept was first demonstrated by E. A. Ash and G. Nicholls (*12*), who attained $\lambda/60$ resolution by using λ = 3 cm microwaves.

To extend these results to visible wavelengths required a reduction in scale of almost five orders of magnitude. Several technical issues had to be addressed for this to be possible, including those of probe formation, mechanical stability, micropositioning, signal manipulation and detection, and distance regulation. Some were first addressed in the development of the Topografiner (*13*), a scanning field emission microscope. NSOM has also benefitted from later developments

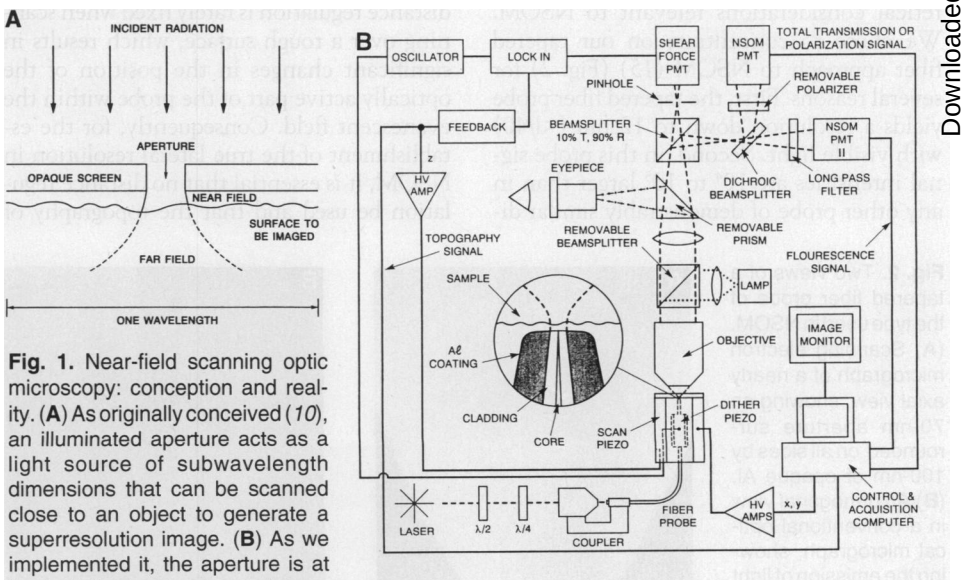

Fig. 1. Near-field scanning optic microscopy: conception and reality. (**A**) As originally conceived (*10*), an illuminated aperture acts as a light source of subwavelength dimensions that can be scanned close to an object to generate a superresolution image. (**B**) As we implemented it, the aperture is at the end of a sharp probe, and shear forces between the tip and sample are measured to automatically control the relative separation for scanning rough surfaces. The scan head is designed as an attachment to a commercial optical microscope, which results in a wide range of possible magnifications. The near-field signal can also be partitioned to obtain information from several contrast mechanisms at once.

in scanning probe microscopy (5, 14), which have accelerated considerably with the advent of STM.

When all the necessary factors have been taken into account, one arrives at a system similar to that shown schematically in Fig. 1B. Here, an NSOM instrument is advantageously built around a conventional optical microscope to permit simultaneous low magnification imaging (up to x1000) and to facilitate optical manipulation of the detected signal. In one embodiment (15), laser light is coupled into a near-field probe formed from an aluminum (Al)-coated, tapered optical fiber. After transmission through both the aperture at the apex of this probe and the sample, the remaining light is collected with an objective lens of the conventional system. The signal can then be partitioned to yield simultaneous data from several complementary contrast mechanisms. A computer is used to synchronize the piezoelectrically generated scanning motion (*16*) to the data acquisition cycle, resulting in the formation of an image on a monitor. In our instrument, shear force distance regulation (*17*) is also used to maintain a fixed probe relative to sample separation, even over a rough surface.

The single most important element in any form of scanning probe microscopy is the probe itself. The probes that have been proposed and applied to NSOM come in three varieties: those that use apertures (*15*, *18–21*), those involving near-field scattering mechanisms (*22–31*), and those dependent on luminescence effects (*32-34*). Some of these techniques have been summarized previously in a review by D. W. Pohl (*35*), which is also an excellent source for theoretical considerations relevant to NSOM. We chose to concentrate on our tapered fiber approach to NSOM (*15*) (Fig. 2) for several reasons. First, the tapered fiber probe yields a resolution down to 12 nm (<l/40) with visible light. Second, in this probe signal intensities are 10^4 to 10^5 larger than in any other probe of demonstrably similar dimensions. This raises the possibility of the investigation of dynamic processes in nearly real time or the imaging of samples exhibiting very weak contrast. Third, the probe is extremely versatile in terms of both the number of optical contrast mechanisms that can be adapted to it and the variety of samples to which it can be applied. Finally, and no less importantly, the tapered fiber probe approach has demonstrated an unmatched level of reliability, so that NSOM is at last sufficiently mature to be applied to a wide range of problems on a routine basis.

Resolution in NSOM

An important step in the development of any new near-field probe is the characterization of its resolution capabilities. Unfortunately, spatial resolution in NSOM is a surprisingly complicated issue, as it is all too easy to generate high spatial frequencies that, upon further analysis, are found not to result from the lateral imaging capabilities of the probe. The sources of this confusion are several. First, the electromagnetic (EM) field within the near field has evanescent components that result in a high degree of sensitivity in the direction normal to the sample. Unless the relative probe to sample separation is kept stable over the entire course of a scan, these components can produce sharp lateral features that reflect only the vertical resolution on a flatter surface, such features would not be observed. An independent distance regulation mechanism is therefore commonly used to stabilize the relative separation. However, this only exacerbates the problem, because the portion of the probe that interacts with the sample to provide distance regulation is rarely fixed when scanning over a rough surface, which results in significant changes in the position of the optically active part of the probe within the evanescent field. Consequently, for the establishment of the true lateral resolution in NSOM, it is essential that no distance regulation be used and that the topography of the test sample be small compared to the limits of the claimed resolution.

Even if these two criteria are met, the interpretation of the resolution can still be difficult. For example, we have observed that even a large probe (> 200 nm) can yield a high degree of sharpness (< 50 nm) on an isolated edge and still be incapable of resolving periodic features of moderate size (~100 nm). In some cases, this can be attributed to surface force interactions between the probe and the sample, of which actual contact is the most crude variety. In other cases, however, it is simply a consequence of the fact that both resolution and contrast in NSOM result from a nonlinear interaction (in the spatial frequency sense) that arises from a complicated set of boundary conditions imposed by the combined probe-sample system. As a result, an unequivocal demonstration of resolution can be achieved only by the imaging of close, packed features previously characterized by a different, well-established technique such as electron microscopy. Furthermore, it must be kept in mind that any such results will depend strongly on the properties of both the sample and the incident EM field (such as, propagation direction, polarization, and wavelength), and different results might be obtained with the same probe under different circumstances.

With only a few exceptions (*12*, *15*, *36*), the above criteria have rarely been met in claims of superresolution in NSOM. An example (*37*) in which they are indeed fulfilled is provided in the images of an electron beam-fabricated test pattern (*38*) (Fig. 3). As the scanning electron micrograph in Fig. 3A demonstrates, electron microscopy remains the method of choice for applications in which its disadvantages can be tolerated. The optical image in Fig. 3B ap-

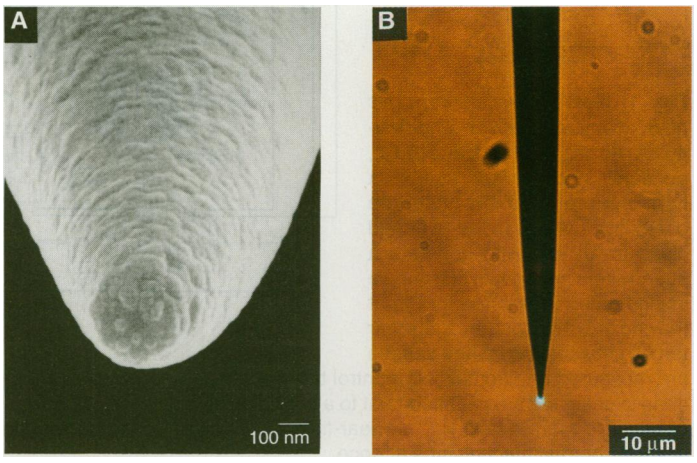

Fig. 2. Two views of a tapered fiber probe of the type used in NSOM. (**A**) Scanning electron micrograph of a nearly axial view, showing an 70-nm aperture surrounded on all sides by 100-nm of opaque Al. (**B**) An orthogonal view in a conventional optical micrograph, showing the emission of light (λ = 488 nm) at the apex.

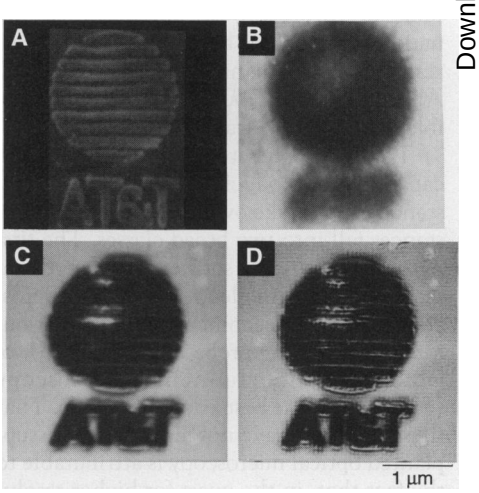

Fig. 3. Resolution comparison of various microscopic methods. (**A**) Scanning electron microscopy. (**B**) Conventional optical microscopy (obtained with a x 100, 0.9 numerical aperture objective). (**C**) Original NSOM data. (**D**) NSOM data after Fourier deconvolution (*37*).

proaches the best resolution obtainable by conventional means (numerical aperture = 0.9), although it clearly conveys little information on the length scale of interest. On the other hand, much more detail is present in the corresponding near-field micrograph (Fig. 3C). Furthermore, if the response of the instrument to a delta function input is known, Fourier deconvolution (8) can be used to compensate for the spatial filtering properties of the microscope, resulting in a reconstruction (Fig. 3D) that highlights the smaller sample features. The caveat must be made, however, that such a reconstruction will not be strictly accurate, because the probe-sample interaction renders NSOM neither linear nor space-invariant, as is required in such a deconvolution.

Results of this order demand that the probe be close to the sample. Several theoretical estimates have been made of the exact separation required (*9, 39–41*); actual experimental results are shown (Fig. 4). As predicted, the highest spatial frequencies decay most rapidly away from the sample, and, with a sufficiently small probe, there is a noticeable loss of information within the first 50 Å. By the time the separation approaches a wavelength, the resolution becomes no better than that attainable by conventional means. From a practical standpoint, these results raise three important questions.

1. *Is subsurface imaging possible?* The achievable resolution degrades with increasing distance from the probe as indicated in Fig. 4. Thus, although it may be possible to obtain superresolution information in three dimensions within a few tens of nanometers of the surface (permitting, for example, an investigation of cytoskeletal organization or the structure and function of membrane-based receptors), more deeply buried structures in transmissive samples are better studied with complementary techniques such as the optical sectioning capabilities of conventional microscopy (42).

2. *Must the sample be thin?* The boundary conditions that exist in the immediate vicinity of the probe play a dominant role in determining both resolution and contrast in NSOM, because they determine the degree to which the EM energy in the near field is coupled out to the far-field detector. Consequently, high-resolution surface information can be obtained in transmission even from thick specimens. Of course, optically perturbative structures at larger distances will also contribute to the observed image, but the desired superresolution component can be isolated by processing either the vertical information (such as in a scan series similar to that in Fig. 4) or the lateral (Fig. 3D). Alternatively, higher spatial frequencies can be amplified during the course of a scan by modulating the probe in either direction (*27,43, 44*).

3. *Must the sample be flat?* Two elements are important here. First, the optically active region of the probe must be at the exact apex of a sharply pointed structure, so that it can reach within recessed regions of rough surfaces. The tapered fiber probe is relatively well suited in this regard, although its outer diameter (200 to 300 nm) still places a limit on the degree of roughness that can be tolerated. This is, however, a problem common to all forms of scanning probe microscopy. Second, a distance regulation mechanism is needed to keep the probe within the near field everywhere over the surface. Several such methods have been employed previously, including point contact (*19*), electron tunneling (*36, 45, 46*), photon tunneling (*22, 24–26*), and capacitance (*36*). Perhaps the best option consists of combining NSOM with surface force feedback (*17, 43, 47*), because force microscopy (*48*) comes the closest of all other scanned probe methods to matching the inherent versatility of NSOM. It must be remembered, however, that the simultaneous use of any distance regulation system can affect the apparent resolution and contrast in NSOM.

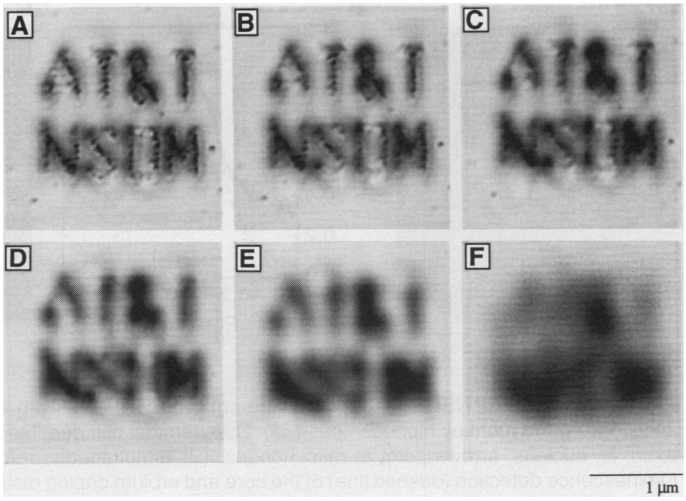

Fig. 4. Resolution in NSOM as a function of the probe-to-sample separation. The separation in each case is **(A)** near contact; **(B)** 5 nm; **(C)** 10 nm; **(D)** 25 nm; **(E)** 100 nm; and **(F)** 400 nm.

Optical Contrast in the Near Field

Several techniques, notably electron microscopy and STM, offer resolution well in excess of the ~12 nm currently achievable in NSOM. Unlike these methods, however, NSOM retains most of the advantages that make conventional optical microscopy the most widespread imaging method in the world today. Chief among these is contrast: optical contrast mechanisms have been refined with centuries of effort, and their analogs, when applicable, are frequently not well developed in other microscopies. As shown in Fig. 5, however, many such mechanisms can be applied to NSOM. In some cases, the resulting contrast is similar to that observed in the far field, whereas in others, uniquely near-field effects are seen. Such effects provide additional sample information but can also complicate the issue of image interpretation.

An example of such complication is shown in Fig. 5A (*15*). Here, the primary contrast mechanism is the opacity of the Al film, which defines this test pattern on a glass substrate. However, the roughness of the Al also has an effect, because the resulting variation in the relative probe to sample separation leads to significant changes in the amount of light that can escape from the aperture. Consequently, the surface structure is accentuated relative to that observable by electron microscopy. Polarization effects, as shown by the brighter sections in the letters A and O, are also involved. These phenomena are most pronounced on opaque metallic patterns, because they result in the most abrupt changes in the requisite boundary conditions. On nonmetallic absorbers (Fig. 6A), the contrast is more frequently akin to that observed in conventional optics.

Polarization contrast (*15, 36, 37, 49, 50*) was also documented on a test pattern consisting of Al rings on glass (Fig. 5B). One advantage of the tapered fiber probe is that the polarization at the aperture, as measured in the far field, can be set to any desired point on the Poincaré sphere, with extinction ratios in excess of 2000:1. Horizontally oriented linear states were chosen at both the aperture and detector to produce the images in Fig. 5B. Two effects were observed. First, when the aperture was over the nominally opaque Al ring in a section perpendicular to the polarization, more light reached the detector than when the aperture was unoccluded. This nonintuitive result represents another example of tip-sample interactions. Second, each ring appeared wider on sections parallel to the electric held polarization than on those perpendicular to it, because it was more difficult to match the boundary conditions (the electric field must be perpendicular to the ring surface) under such circumstances, therefore causing the

aperture transmission to be affected over a longer range. This further illustrates the difficulty of arriving at a simple definition of resolution in NSOM.

It is also possible to generate near-field contrast from the real part of the refractive index (*22*, *37*, *51*), as demonstrated in the image of a test pattern exposed and developed into a polymethylmethacrylate film (Fig. 5C). The contrast results solely from refractive index-induced changes in the coupling of light from the aperture. Such results might be useful for the imaging of low-contrast biological objects or for line width inspection during the fabrication of integrated circuits. It should also be possible to use the near-field optical path as one leg of an interferometer to accomplish true near-field phase microscopy.

From the perspective of biology, fluorescence may be the most powerful contrast mechanism, because a wide variety of site-specific fluorescent probes have been developed, including some with emission sensitive to the local environment (such as, pH or Na^+ concentration). The extension of fluorescence to the near field (*21*, *37*, *46*, *51*–*54*) is demonstrated in Fig. 5D. The sample consists of polystyrene beads with a mean diameter of 51 nm, some of which were infused with a green dye and others with an orange-red one. The image shown is a composite of two micrographs, each taken with a wavelength selective filter to distinguish which dye was incorporated in each bead. This multiple color imaging capability might be combined with, for example, fluorescence in situ hybridization techniques for gene mapping (*55*) or for oncological studies through observation of chromosome abnormalities (*56*). High sensitivity is also demonstrated in Fig. 5D, as the orange-red beads contained on average ~200 dye molecules and the absorption at the excitation wavelength was almost two orders of magnitude removed from the maximum, therefore suggesting a potential detection limit of a few molecules. Such sensitivity may be aided by near-field effects such as enhanced fluorescence (*51*, *57*) from intense EM fields at the excitation wavelength in the vicinity of the probe and reduced background luminescence resulting from the smaller effective excitation volume.

All the results presented thus far were obtained in a near-field transmission configuration. NSOM is also readily adapted to a reflection geometry (*20*, *22*, *23*, *37*, *58*–*60*) for the high-resolution imaging and spectroscopic probing of opaque samples. In the simplest such adaptation, a long working distance objective is placed concentric with the probe on the same side of the sample. By analogy to transmission NSOM, either the reflection-illumination or the reflection-collection mode can be used. The former configuration was used to obtain the results shown (Fig. 5, E and F).

It is frequently desirable to obtain an entire emission or excitation spectrum from a localized region. The ability to obtain such data is demonstrated in Fig. 5E, where the room temperature luminescence spectrum of a GaAs/AlGaAs heterostructure is presented. The sample ws excited with a few nanowatts of light ($\lambda = 514$ nm) through a fiber probe, and the efficiency of the system was such that, even with this rather weakly emitting sample, a specturm with a good signal-to-noise ratio could be taken with an integration time of 1 s. On most samples, it should be possible to take a 100 × 100 pixel image with a spectrum at each point in ~1 hour. We have obtained similar spectra in the collection mode (*36*, *49*, *61*) with somewhat lower efficiency; it remains to be seen if this difference is fundamental. It is important to be able to operate in both modes because they are not symmetric (50). For example, an illumination mode spectrum will contain information from emission events throughout the diffusion volume of the excitations created locally under the probe, whereas a collection mode spectrum will be heavily weighted toward emission very near the probe. However, when photochemical degradation of the specimens is an issue, the measurement is best performed in the illumination mode, as the excitation light then illuminates only an aperture-sized region at any time.

An example of imaging in the reflection mode is presented in Fig. 5F. The Al pattern in this example appears brighter than the

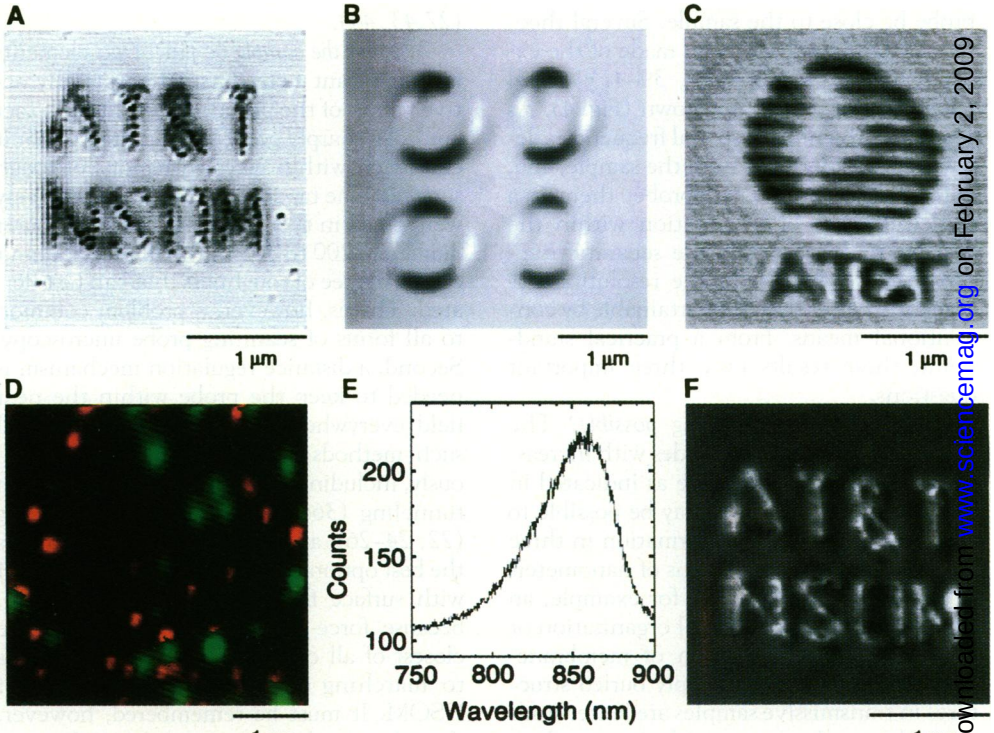

Fig. 5. Extension of optical contrast mechanisms to the near field. (**A**) Absorption (**15**). (**B**) Polarization (50). (**C**) Refractive index. (**D**) Two-color fluorescence. (**E**) Spectroscopy. (**F**) Reflectivity.

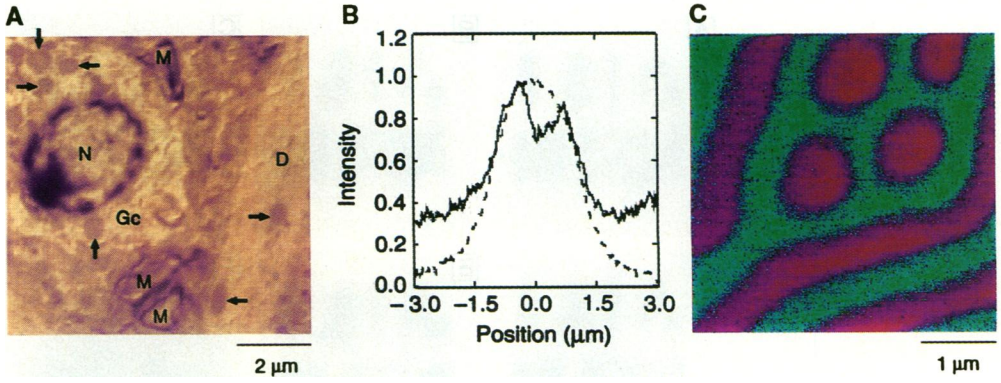

Fig. 6. Applications of NSOM, each with a different contrast mechanism. (**A**) Absorption within a tissue section from the monkey hippocampus (*62*). D, pyramidal cell dendrite; Gc, glia cell; M, myelinated axon; N, nucleus; arrows point at mitochondria. (B) Simultaneous refractive index (solid line) and luminescence detection (dashed line) of the core and erbium doping distribution within an optical fiber (*37*). (**C**) Polarization imaging of magnetic domains within a bismuth-doped, yttrium-iron-garnet film.

glass substrate as a result of its highter reflectivity. Refractive index and fluorescence contrast have been adapted to reflection NSOM, but polarization contrast is adversely affected in the reflection-illumination mode by scattering of light at the edges of the probe. This problem might be avoided, however, if the probe can be adapted to simultaneous illumination and collection.

Applications of NSOM

The most important consequence of our ability to extend the power of optical contrast mechanisms to the near-field regime is that it leads to a technique of considerable versatility. This is demonstrated by the applications presented in Fig. 6, in which the essential information in each case was obtained with a different contrast mechanism.

In the field of optical pathology, contrast is generated in thin tissue sections with a variety of well-developed absorptive stains. The resulting specimens can therefore be imaged without further modification by means of NSOM. This is demonstrated in Fig. 6A on a specimen taken from the hipocampus of the monkey brain. The original tissue sample was fixed with glutaraldehyde and embedded in epon for sectioning (*62*). A toludin blue-stained, 80-nm-thick section was imaged in Fig. 5A; yet, the stain was both sufficiently absorptive and selective to reveal features on a scale previously accessible only to transmission electron microscopy (TEM). UnlikeTEM, however, the simultaneous use of NSOM with conventional optical microscopy (Fig. lB) permits the magnification to be changed easily from < ×100 to > ×50,000, so that a small region can be quickly identified in relation to its surroundings. Furthermore, image interpretation in this application is straightforward, because the near-field contrast is similar to that observed in the far field. Indeed, this point was emphasized in Fig. 6A by the use of a false color table to mimic the colors normally seen by conventional optical microscopy. These advantages, coupled with its ease of use and substantially lower cost, indicate that NSOM may prove to be a useful tool in clinical pathology. Our primary motivation, however, is that the imaging of tissue sections represents a logical first step in the application of NSOM to biology and may eventually lead to the investigation of more complex biological systems.

In some applications, it is necessary or desirable to obtain information from two or more contrast mechanisms at once. An example is shown in Fig. 6B (*37*) in line scans extracted from NSOM images of an ~500-nm-thick section of an erbium-doped optical fiber (*63*). Er fibers are currently being used as optical amplifiers and fiber lasers (*64*) and will likely be employed in the next generation of transoceanic telecommunications lines. However, variations in the exact distribution of Er relative to the fiber core can significantly affect the gain and optimal length of a fiber amplifier, and thus a technique is needed to visualize both the core and the Er distribution with submicron resolution. Refractive index contrast in NSOM allows the core to be profiled, whereas luminescence at λ = 1.5 μm can be used to measure the Er distribution. In the particular case in Fig. 6B, the Er clearly exists throughout the core, with a significant amount of spreading to the cladding beyond. High sensitivity is also needed in this application: the refractive index difference between the core and the cladding is only about 3%, the Er doping density is less than or equal to 0.1%, and the absorption cross section of an Er ion is ~ $\times 10^5$ smaller than that of the individual dye molecules within the fluorescent beads in Fig. 5. Although the sensitivity in Fig. 6B is clearly satisfactory, even greater sensitivity may be achievable by operating near a plasmon resonance within the metal coating, as has been proposed in experiments with an aperture in a planar film (*51*). In addition, NSOM can also be used to characterize other light wave device parameters such as the near-field emission profiles from single-mode optical fibers (*65*) and semiconductor lasers (*66*).

In some applications, only polarized light microscopy can generate the necessary contrast. A case in point is in the imaging of magneto-optic (MO) samples, where the polarization of incident light is rotated slightly in the plane perpendicular to the local sample magnetization. This technique can be readily extended to the near field (*37, 50, 67*) by the selection of a linear polarization state at the aperture and by the use of a polarizer before the detector to determine the magnitude and direction of rotation. An example is shown in Fig. 6C on an ~1-μm-thick, bismuth-doped, yttrium-iron-garnet film (*68*). This sample was prepared with uniaxial anisotropy so that domains were formed within the film with magnetization either up or down, and both stripe and bubble-type domains can be seen. False colors were selected to label the domains of opposite magnetization and to highlight the domain boundaries. There are a number of fundamental issues which might be addressed by the application of NSOM to such samples, including the energetics of spin interactions within the domain walls and the mechanisms of domain wall nucleation. Other, technological applications will be discussed below.

With the comparatively large photon flux now available (*15*), NSOM can also be applied to the localized optical modification of surfaces. An obvious application in this area involves superresolution optical lithography, because the line width demands of the semiconductor industry are taxing the capabilities of optical lithography, even with ultraviolet sources. Indeed, the ability to use near-field methods to replicate optically evanescent spatial frequencies in photoresist or a bleachable dye layer was convincingly demonstrated (*69,70*) even before the first efforts at near-field optical imaging. A more recent approach (Fig. 7A) uses a tapered fiber probe with shear force distance regulation to permit near-field exposures even on the rough surfaces normally encountered during device fabrication. To generate the pattern in Fig. 7A, an ~50-nm-thick film of conventional optical photoresist was exposed with 1-ms pulses at an input power within the fiber of ~80 μW at λ = 420 nm and developed for 25 s with a standard developer. Lines and spaces down to ~100 nm were easily produced. The demonstrated sensitivity is sufficient so that the write speed will not be limited by the flux but rather by the mechanical resonances associated with scanning. Hence, the technique is unlikely to be speed-competitive with emerging parallel exposure technologies such as x-ray lithography. Furthermore, work is also needed to demonstrate that practical device processing can be performed in near field-exposed, thin-resist layers. On the other hand, the method is simple and inexpensive and might be combined with simultaneous NSOM imaging at a resist-insensitive wavelength to provide automatic alignment in multiple-step processing routines or to pro-

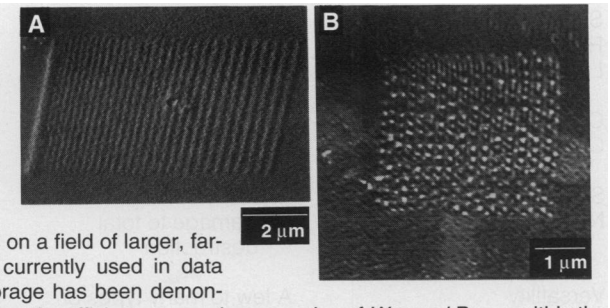

Fig. 7. Surface modification with NSOM. (A) Line widths and spaces down to ~ 100 nm exposed and developed in a commercial photoresist film. Lithography on this scale will be required to reach integrated circuit capabilities projected for the turn of the century. (**B**) An array of MO domains written and imaged by means of NSOM, superimposed on a field of larger, far-field written domains of the type currently used in data storage applications. Near-field storage has been demonstrated at densities up to ~45 Gbits/inch^2, sufficient to encode two copies of *War and Peace* within the area of an average character in this sentence.

vide closed-loop control of the lithographic process through the in situ measurement of exposure-induced changes in the refractive index of the resist. Consequently, near-field lithography may indeed find uses in some specialized areas that are currently the province of electron beam lithography.

An application that uses both the surface modification and imaging capabilities of NSOM is in the field of high-density data storage. In fact, conventional optics plays a central role in data storage formats such as compact disc read-only memory (CD-ROM), write once-read many (WORM) memory, and erasable optical memories that use either MO or reversible phase-change media. However, the bit dimensions and storage densities of optical drives are already at the limits imposed by diffraction. With NSOM, on the other hand, MO storage has been demonstrated at densities ~×100 greater than in currently available magnetic or far-field optical technologies (67). For example, the large, dim circles in the background of Fig. 7B represent individual bits written in an MO film (a cobalt-platinum multilayer) with far-field optics and imaged by means of polarization contrast NSOM as described above. The array superimposed over this was written in the near field by pulsing a second, higher power beam through the tapered fiber probe to locally heat the film near the Curie temperature, which resulted in the formation of a small domain of opposite magnetization. Thus far, individual domains of ~60-nm diameter have been generated, as have packing densities of ~45 Gbits/inch^2 (67). Of course, other parameters such as read-write speed and reliability are also of critical importance, so it remains to be seen if the competing requirements of these parameters will still allow near-field MO storage to find commercial applications.

Future Directions

Although NSOM is conceptually the oldest form of scanning probe microscopy (*10*), experimental efforts at optical frequencies have begun only within the last decade. Consequently, there exist numerous opportunities for continued research, such as in the following areas.

Probe design. Although the tapered fiber probe has led to a resolution down to ~12 nm for λ = 514 nm, further resolution improvements in this or in any other strictly aperture-based system are unlikely, because the finite opacity of the Al coating that defines the aperture limits the degree to which light can be confined. Indeed, by modeling the evanescent EM modes within the aperture, one can estimate the optimum confinement for λ ~500 nm to occur for a 20-nm-diameter aperture, yielding a 30-nm full width at the half-maximum impulse response function and a high frequency cutoff in the transfer function corresponding to ~12-nm resolution at the signal-to-noise ratios typically encountered. These values are in good agreement with experimental results (*15*). Although this resolution is sufficient for a wide range of applications, in certain disciplines, such as molecular biology, even higher resolution is essential.

Two major approaches are currently under investigation with this in mind. Luminescent probes use either a luminescent material within an aperture in an attempt to minimize the resolution and signal problems associated with evanescence (*32, 34*) or an isolated luminescent particle that acts as a light source of subwavelength dimensions (*33*). With this latter system, a single luminescent ion could, in principle, be scanned a few angstroms above a surface to achieve near-atomic resolution. The second method involves isolating the near-field component of the scattering from a sharp probe, such as through surface-enhanced Raman scattering from a Ag tip (*31*), heterodyne detection from an oscillating STM-type probe (*27*), frustrated total internal reflection with a glass fiber (*24–26*), or resonant plasmon-enhanced scattering from a surface (*30, 51*) or protrusion (*23, 28, 29*). Although all of these approaches are potentially fruitful, in each case there are both practical and fundamental problems to be dealt with, and resolution superior to the tapered fiber probe has yet to be unequivocally demonstrated.

Even if higher resolution can be achieved, however, the history of microscopy is ample reminder of the fact that resolution is far from the only important parameter to be considered. Several other relevant features are listed in Table 1, along with the useful range in each case and the current performance of the tapered fiber probe. Thus, for example, although the current resolution of <~λ40 is considerably better than the ~λ/2 limit of conventional optics, it does not approach the ~λ/2000 level needed for atomic resolution. Any further advances in one area, such as resolution, will likely come at the expense of several others, such as signal and versatility. Indeed, the tapered fiber probe itself represents a compromise in this regard, albeit a successful one consciously arrived at in order to secure the broadest possible applicability for the technique.

Theory. To guide the continued development of new probes and to understand fully the contrast mechanisms involved in NSOM, researchers will need theoretical models of the near field. Such models have already advanced from the comparatively simple case of an aperture in a thin, conducting screen (*40, 71, 72*), to one in a screen of arbitrary thickness (*73*), to one at the end of a conical probe (*74*). At the same time, researchers have worked to model tip-sample interactions by solving Maxwell's equations in a rudimentary slit-on-slit geometry (*36, 75*), by investigating Laplace's equation for a hyperbolic probe near a flat surface (*76*), and by using a self-consistent multipolar approach for a dielectric sphere near a dielectric surface (*77*). Unfortunately, the problems of practical interest involve systems far more complicated than these, and, considering the extreme sensitivity observed experimentally to a variety of parameters (such as the tip and sample material properties, the exact geometry of the combined system, and the nature of the incident EM field), it is not yet clear that realistic models, if attainable, will be of sufficient generality to be truly useful.

Applications. The examples given in Figs. 6 and 7 represent only a small fraction of the systems to which NSOM might be fruitfully applied. In the area of semiconductor technology, possible applications include mask inspection and repair; refractive index imaging of latent (that is, exposed but undeveloped) features in photoresist; localized pho-

Table 1. Parameters relevant to probe design in NSOM and current performance of the tapered fiber probe.

Parameter	Useful range	Current performance
Resolution	λ/2 to λ/2000	<λ/40
Signal	10 photons/s to 10 mW	>50 nW (80-nm aperture)
Reliability	10 to 100%	~90%
Lifetime	Storage: 1 day to 1 year	>3 months
	Usage: 1 min to 1 year	>3 days
Cost	0 to $1000	~$10
Contrast	One type to many	Six shown in Fig. 5; more possible
Spectral range	<200 nm to 10 μm	~300 nm to ~2 μm
Nondestructiveness	No damage to total destruction	Good; only problem is heating at higher powers
Versatility	A few to many types of samples	Good; except probe shape limits permissible surface roughness

toconductivity measurements; and intensity profiling of light wave devices. In more fundamental areas of solid-state physics, near-field spectroscopy, particularly at low temperatures, could contribute to investigations of quantum-confined structures, dopant distributions and diffusion, and exciton interactions with single impurities. Materials issues in structurally heterogeneous media such as liquid crystals, self-assembled monolayers, and block copolymers could also be studied. In the biological arena, fluorescence NSOM coupled with photobleaching recovery measurements or correlation spectroscopy could yield small-scale diffusion data. Perhaps most exciting, however, is the potential for nondestructive, high-resolution fluorescence imaging of living cells in their native environments. For example, individual membrane channels and receptors might be imaged, along with their regulation of ion and chemical flow. Such activity might then be correlated to simultaneous patch-clamp data and force measurements of mechanical transduction. With the recent combination of NSOM with force-based distance regulation, such problems may be amenable to treatment in the near future.

REFERENCES AND NOTES

1. An overview of physics and engineering on the nanometric scale can be found in a special section of *Science* **254**, 1300–1342 (29 November 1991).
2. E. Abbe, *Archiv. Mikros. Anat.* **9**, 413 (1873).
3. D. F. Parsons, Ed., *Short Wavelength Microscopy* (New York Academy of Sciences, New York, 1978).
4. D. Sayre, Ed., *X-ray Microscopy II: Proceedings of the Second International Symposium* (Springer-Verlag, New York, 1988).
5. H. K. Wickramasinghe, Ed., *Scanned Probe Microscopy* (American Institute of Physics, New York, 1992).
6. G. Binnig, H. Rohrer, Ch. Gerber, E. Weibel, *Phys. Rev. Lett.* **49**, 57 (1982).
7. Over a dozen different names and acronyms have been attached to near-field microscopy at one time or another, but near-field scanning optical microscopy (NSOM; pronounced EN-som) and scanning near-field optical microscopy (SNOM) are the ones in most frequent usage.
8. J. W. Goodman, *Introduction to Fourier Optics* (McGraw-Hill, New York, 1968).
9. G. A. Massey, *Appl. Opt.* **23**, 658 (1984).
10. E. H. Synge, *Phil. Mag.* **6**, 356 (1928).
11. The near-field concept has been independently formulated by several researchers, but E. H. Synge's work was first brought to the attention of the near-field community by D. McMullan [*Proc. R. Microsc. Soc.* **25**, 127 (1990)].
12. E. A. Ash and G. Nicholls, *Nature* **237**, 510 (1972).
13. R. Young, J. Ward, F. Scire, *Rev. Sci. Instr.* **43**, 999 (1972).
14. D. W. Pohl, *IBM J. Res. Dev.* **30**, 417 (1986).
15. E. Betzig, J. K. Trautman, T. D. Harris, J. S. Weiner, R. L. Kostelak, *Science* **251**, 1468 (1991).
16. G. Binnig and D. P. E. Smith, *Rev. Sci. Instr.* **57**, 1688 (1986).
17. E. Betzig, P. L. Finn, J. S. Weiner, *Appl. Phys. Let.* **60**, 2484 (1992).
18. A. Lewis, M. Isaacson, A. Harootunian, A. Murray, *Ultramicroscopy* **13**, 227 (1984).
19. D. W. Pohl, W. Denk, M. Lanz, *Appl. Phys. Lett.* **44**, 651 (1984).
20. U. Ch. Fischer, *J. Vac. Sci. Technol.* B3, 3861 (1985).
21. E. Betzig, A. Lewis, A. Harootunian, M. Isaacson, E. Kratschmer, *Biophys. J.* **49**, 269 (1986).
22. D. W. Pohl, U. Ch. Fischer, U. T. Dürig, *Proc. Soc. Photo-Opt. Instrum. Eng.* **897**, 94 (1988).
23. U. Ch. Fischer and D. W. Pohl, *Phys. Rev. Lett.* **62**, 458 (1989).
24. R. C. Reddick, R. J. Warmack, T. L. Ferrell, *Phys. Rev.* **B39**, 767(1989).
25. D. Courjon, K. Sarayeddine, M. Spajer, *Opt. Commun.* **71**, 23 (1989).
26. F. de Fornel, J. P. Goudonnet, L. Salomon, E. Lesniewska, *Proc. Soc. Photo-Opt. Instrum. Eng.* **1139**, 77 (1989).
27. H. K. Wickramasinghe and C. C. Williams, U.S. Patent 4 947 034 (1990)
28. U. Ch. Fischer, paper presented at the International Conference on Scanning Tunneling Microscopy, Interlaken, Switzerland, 12 – 16 August 1991 .
29. S. Schultz and T. J. Silva, paper presented at the conference Scanning Probe Microscopies, Society of Photo-Optical Instrumentation Engineers, Los Angeles, CA, 19–25 January 1992.
30. M. Specht, J. D. Pedarnig, W. M. Heckl, T. W. Hansch, *Phys. Rev. Lett.* **68**, 476 (1992).
31. J. Wessel, *J. Opt. Soc. Am.* **B2**, 1538 (1985).
32. K. Lieberman, S. Harush, A. Lewis, R. Kopelman, *Science* **247**, 59 (1990).
33. E. Betzig and J. K. Trautman, U.S. Patent 5 105 305 (1992).
34. A. Lewis and K. Lieberman, *Nature* **354**, 214 (1991).
35. D. W. Pohl, in *Advances in Optical and Electron Microscopy*, C. J. R. Sheppard and T. Mulvey, Eds (Academic Press, London, 1990), pp. 243–312.
36. E. Betzig, thesis, Cornell University (1988).
37. J. K. Trautman *et al.*, *J. Appl. Phys.* **71**, 4659 (1992).
38. All electron beam fabrication test patterns in this work were supplied by J. S. Weiner, AT&T Bell Laboratories.
39. E. Betzig, A. Harootunian, A. Lewis, M. Isaacson, *Appl. Opt.* **25**, 1890 (1986).
40. Y. Leviatan, *J. Appl. Phys.* **60**, 1577 (1986).
41. E. Marx and E. C. Teague, *Appl. Phys. Lett.* **51**, 2073 (1987).
42. Several articles on three-dimensional optical image reconstruction can be found in *New Methods in Microscopy and Low Light Imaging*, J. E. Wampler, Ed. (Society of Photo-Optical Instrumentation Engineers, Bellingham, WA, 1989).
43. R. Toledo-Crow, P. C. Yang, Y. Chen, M. Vaez-Iravani, *Appl. Phys. Lett.* **60**, 2957 (1992).
44. M. A. Paesler, C. Johnson, P. J. Moyer, E. Buckland, C. Jahncke, paper presented at the conference Scanning Probe Microscopies, Society of Photo-Optical Instrumentation Engineers, Los Angeles, CA, 19–25 January 1992.
45. U. Durig, D. W. Pohl, F. Rohner, *J. Appl. Phys.* **59**, 3318 (1986) .
46. A. Harootunian, E. Betzig, M. Isaacson, A. Lewis, *Appl. Phys. Lett.* **49**, 674 (1986).
47. N. F. van Hulst *et al.*, paper presented at the conference Scanning Probe Microscopies, Society of Photo-Optical Instrumentation Engineers, Los Angeles, CA, 19–25 January 1992.
48. G. Binnig, C. F. Quate, Ch. Gerber, *Phys. Rev. Lett.* **56**, 930 (1986).
49. E. Betzig, M. Isaacson, H. Barshatzky, A. Lewis, K. Lin, *Proc. Soc. Photo-Opt. Instrum. Eng.* **897**, 91 (1988).
50. E. Betzig, J. K. Trautman, J. S. Weiner, T. D. Harris, R. Wolfe, *Appl. Opt.*, in press.
51. U. Ch. Fischer, *J. Opt. Soc. Am.* **B3**, 1239 (1986).
52. S. Okazaki, H. Sasatani, H. Hatano, T. Hayashi, J. Nakamura, *Mikrochim. Acta* **3**, 87 (1988).
53. A. Lewis, E. Betzig, A. Harootunian, M. Isaacson, E. Kratschner, in *Spectroscopic Membrane Probes*, L. M. Loew, Ed. (CRC Press, Cleveland, 1988), pp. 81–110.
54. M. A Paesler *et al.*, *Phys. Rev.* **B42**, 6750 (1990); P. J. Moyer, C. L. Jahncke, M. A. Paesler, R. C. Reddick, R. J. Warmack, *Phys. Lett.* **A145**, 343 (1990).
55. J. B. Lawrence, R. H. Singer, J. A. McNeil, *Science* 249, 928 (1990).
56. D. Pinkel, T. Straume, J. W. Gray, *Proc. Natl. Acad. Sci. U.S.A.* **83**, 2934 (1986).
57. D. A. Weitz, S. Garoff, J. I. Gersten, A. Nitzan, *J. Chem. Phys.* **78**, 5324 (1983).
58. U. Ch. Fischer, U. T. Dürig, D. W. Pohl, *Appl. Phys. Lett.* **52**, 249 (1988).
59. D. Courjon, J. Vigoureux, M. Spajer. K. Sarayeddine, S. Leblanc, *Appl. Opt.* 29, 3734 (1990).
60. J. A. Cline, H. Barshatzky, M. Issacson, *Ultramicroscopy* **38**, 299 (1991).
61. E. Betzig, M. Isaacson, A. Lewis, *Appl. Phys. Lett.* **51**, 2088 (1987).
62. Work in collaboration with F. Naftolin, L. M. Gosegura, and C. Leranth, Department of Obstetrics and Gynecology, Yale University School of Medicine.
63. Work done in collaboration with D. J. DiGiovanni, AT&T Bell Laboratories.
64. Special issue on optical amplifiers, *J. Lightwave Technol.* **9** (February 1991).
65. D. J. Butler, K. A. Nugent, A. Roberts, P. D. Kearney, *Proc. Soc. Photo-Opt. Instrum. Eng.* **1556**, 19 (1991).
66. M. Isaacson, J. Cline, H. Barshatzky, in *Scanned Probe Microscopy*, H. K. Wickramasinghe, Ed. (American Institute of Physics, New York, 1992) pp. 23–36.
67. E. Betzig, J. K. Trautman, R. Wolfe, E. M. Gyorgy, P. L. Finn, M. H. Kryder, C.-H. Chang, *Appl. Phys. Lett.*, in press.
68. Sample courtesy of R. Wolfe, AT&T Bell Laboratories.
69. U. Ch. Fischer and H. P. Zingsheim, *J. Vac. Sci. Technol.* **19**, 881 (1981).
70. U. Ch. Fischer and H. P. Zingsheim, *Appl. Phys. Lett.* **40**, 195 (1982).
71. H. A. Bethe, *Phys. Rev.* **66**, 163 (1944).
72. C. J. Bouwkamp, *Philips Res. Rep.* **5**, 401 (1950).
73. A. Roberts, *J. Appl. Phys.* **65**, 2896 (1989).
74. ———, *ibid.* **70**, 4045 (1991).
75. Y. Leviatan, *IEEE Trans. Microwave Theory and Tech.* **36**, 44 (1988).
76. W. Denk and D. W. Pohl, *J. Vac. Sci. Technol.* **B9**, 510 (1991)
77. C. Girard and D. Courjon, *Phys. Rev.* **B42**, 9340 (1990).

78. We wish to acknowledge, in addition to the collaborations mentioned above, the valuable contributions of T. D. Harris and H. Hess.